Progress In Electromagnetics Research M, Vol. 106, 205–214, 2021

Spatially Squeezed Electromagnetic Modes of a Transformational Optics Based Cavity Resonator for Targeted Material Heating

Barakathulla Asrafali, Chakravarthy Venkateswaran, and Natesan Yogesh*

Abstract—Confining electromagnetic (e-m) modes in a tiny space is a desirable aspect for many applications including targeted material heating and light harvesting techniques. In this work, we report spatially squeezed e-m modes of a cavity resonator formed by the modified transformation optical (TO) medium. The proposed coordinate transformation scheme suggests curved contours of refractive index profile such that the e-m mode can be confined within the contours. The effective mode area for a TO cavity is at least 10 times smaller than the air-filled metallic cavity. The confined e-m modes of a proposed cavity are horizontally flattened but vertically squeezed of the dimension of $\lambda/49$. The material parameters of the proposed TO medium are approximated with non-magnetic and isotropic dielectric values. For an application aspect, squeezed mode of the TO cavity is used for targeted material heating, and it is demonstrated based on e-m thermal co-simulations. A tiny dielectric material placed at the squeezed part of the cavity mode is heated rapidly with the temperature rise of 2.35°C/s (11°C/s) for the single (dual) e-m source excitation with the peak electric field strength of 5×10^4 V/m. We further discuss how one can realize the proposed TO medium practically with a cell-grid approximation using photonic crystals and metamaterials.

1. INTRODUCTION

Confining electromagnetic (e-m) radiation in a tiny space is central in several applications such as targeted heat treatment of biological cells, material characterization, and quantum optics. For example, a cavity mode with low mode-volume/effective mode area represents highly localized state. Such a localized state is essential for improving the emitter-field coupling interactions and controlling spontaneous emission rate in quantum systems [1].

The e-m wave confinement due to spatial compression can be achieved through cavity resonators ranging from metallic enclosure, quantum dots, dielectric resonators to cavities formed by artificial e-m structures such as metamaterials [2, 3] and photonic crystals [4]. For instance, a material with high dielectric constant such as $BaTiO_3$ can be used for achieving spatially compressed e-m modes in the form of dielectric resonators [5]. However, the increase in the dielectric permittivity of a material is not a stand-alone criterion to achieve e-m mode confinement in small volumes, as losses associated with high dielectric permittivity preclude the confinement applications. Instead of finding a material with a high dielectric constant, one can try to explore sub-wavelength spatial variation of dielectric function for tight e-m wave confinement using transformation optics (TO) [6, 7].

Transformation optics uses the principle of form invariance of Maxwell's equations under coordinate transformation, where the transformed space with desired size and shape can show exotic e-m phenomena [8–12]. Several fascinating outcomes of TO devices such as square cloak [13], spherical cloak [14], e-m concentrator [15], beam steering device [16], e-m beam compressor [17], perfect lenses [18], optical black hole [19], optical wormholes [20], wave tilter [21, 22], retro directive reflectors [23], and

Received 18 October 2021, Accepted 17 December 2021, Scheduled 27 December 2021
* Corresponding author: Natesan Yogesh (yogesh_frs@yahoo.co.in).
The authors are with the Department of Nuclear Physics, University of Madras (Guindy Campus), Chennai 600025, India.

optical wave dividers [24] were reported previously. Significant attention has been paid to the concept of e-m beam concentration in tiny volumes using TO devices in the photonics research.

In the present work, we report the formation of squeezed e-m modes in a cavity resonator formed by the modified TO medium. In our realization, the gradient index profile of the TO medium, which has a spatial curvature feature is used for obtaining the spatially squeezed e-m modes. We have observed that the realized TO cavity supports e-m modes with a mode area at least ten times smaller than the conventional air-filled metallic cavity. The e-m mode of TO cavity is horizontally flattened but tightly confined along the vertical direction such that the computed full-width at half-maximum (FWHM) along vertical direction is $\lambda/49$, where λ is the resonant wavelength of the TO cavity.

The practical realization of a TO based device is a major challenge across the entire e-m spectra as TO devices are suffering from strong anisotropy and inhomogeneity nature of the transformed space. To overcome the non-practical values for the material parameters, conformal optical transformation [25] and quasi conformal approach [26] have been proposed previously, which were expected to eliminate the pole problem (the point at which permittivity value is blowing/unbound) in the transformation space. However, the conformal approach can be utilized only if the transformation equation satisfies the Laplace equation, and the quasi conformal mapping still suffers from a pole problem. In our work, the proposed transformation is not a conformal one as it does not satisfy Laplace equation. Hence to avoid singularities in the transformed space, trigonometric functions (sines/cosines) are incorporated in the coordinate transformation. Secondly to avoid non-practical values of transformed parameters, we have approximated the derived TO medium to be non-magnetic and restricted only with the spatial variation of dielectric parameter in the realization. Particularly, dielectric parameters of the TO medium are scaled down by a factor of 10 in order to realize the concept practically.

In second part of the work, electromagnetic thermal co-simulations are carried out to reveal the application aspect of the proposed TO cavity, where a tiny dielectric object loaded at the confinement area of the cavity mode results in rapid heating for single and multiple e-m sources excited outside the cavity. Finally, the discussion on the practical implementation of the TO cavity is presented with respect to cell-approximation scheme, and cavity mode confinement is verified through full-wave e-m calculations.

2. DESIGN PRINCIPLE OF THE PROPOSED OPTICAL TRANSFORMATION

Figure 1 shows the scheme of the proposed coordinate transformation (CT) described by

$$x' = x; \quad y' = y\left(1 - \sin\left(x^2 - \frac{y^2}{b}\right)\right); \quad z' = z, \tag{1}$$

where x and y, and x' and y' are the coordinates of a non-transformed rectangular air space (Fig. 1(a)) and a transformed TO space (Fig. 1(b)), respectively. Here x and z are unchanged. By only transforming the y-coordinates, a valley-like wrapped structure is obtained in Fig. 1(b).

It is useful to mention that the proposed transformation has a sinusoidal function with quadratic powers of x and y with a dimensionless control parameter b. Such incorporation of oscillatory function with the argument $(x^2 - \frac{y^2}{b})$ results in both space compression and stretching depending on x and y values. In the present case, x and y ranges are chosen as $-10 \le x \le 10$ and $-10 \le y \le 10$ so that the transformation space spreads out as $-10 \le x' \le 10$ and $-20 \le y' \le 20$ as shown in Fig. 1(b).

Since Maxwell's equations are form invariant, the proposed scheme corresponds to the following constituent parameters of the TO medium;

$$\varepsilon_{xx} = \frac{b}{b - b \cdot \sin\left(\dfrac{b \cdot x^2 - y^2}{b}\right) + 2 \cdot y^2 \cdot \cos\left(\dfrac{b \cdot x^2 - y^2}{b}\right)} \tag{2}$$

$$\varepsilon_{xy} = -\frac{2 \cdot b \cdot x \cdot y \cdot \cos\left(x^2 - \dfrac{y^2}{b}\right)}{b - b \cdot \sin\left(\dfrac{b \cdot x^2 - y^2}{b}\right) + 2 \cdot y^2 \cdot \cos\left(\dfrac{b \cdot x^2 - y^2}{b}\right)} \tag{3}$$

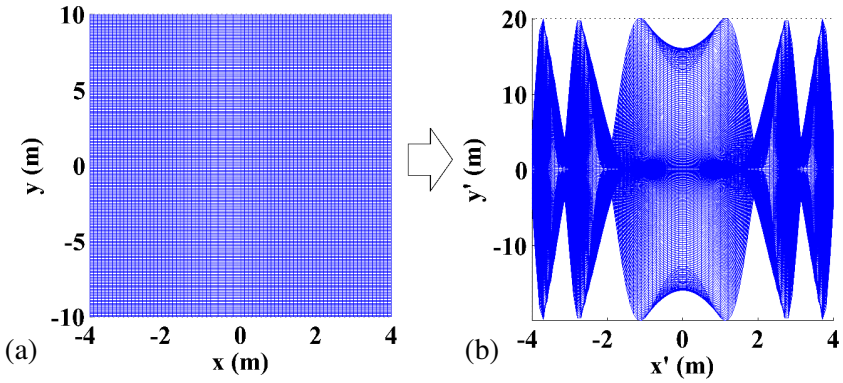

Figure 1. Transformation scheme, (a) rectangular air space, (b) transformed space under CT.

$$\varepsilon_{xz} = 0 \tag{4}$$

$$\varepsilon_{yx} = \varepsilon_{xy} \tag{5}$$

$$\varepsilon_{yy} = \frac{b \cdot \left(\left(\frac{2 \cdot y^2 \cdot \cos\left(x^2 - \frac{y^2}{b}\right)}{b} \right) - \sin\left(x^2 - \frac{y^2}{b} + 1\right) \right) + 4 \cdot x^2 \cdot y^2 \cdot \cos\left(x^2 - \frac{y^2}{b}\right)^2}{b - b \cdot \sin\left(\frac{b \cdot x^2 - y^2}{b}\right) + 2 \cdot y^2 \cdot \cos\left(\frac{b \cdot x^2 - y^2}{b}\right)} \tag{6}$$

$$\varepsilon_{yz} = 0, \tag{7}$$

$$\varepsilon_{zx} = \varepsilon_{xz}, \tag{8}$$

$$\varepsilon_{zy} = \varepsilon_{yz}, \tag{9}$$

$$\varepsilon_{zz} = \varepsilon_{xx} \tag{10}$$

The above constituent parameters correspond to a tensor of rank 2 with 9 components. Here off-diagonal elements such as ε_{xz}, ε_{yz}, ε_{zy} and ε_{zx} are zero, and the permittivity tensor governing the TO medium is $\begin{pmatrix} \varepsilon_{xx} & \varepsilon_{xy} & 0 \\ \varepsilon_{yx} & \varepsilon_{yy} & 0 \\ 0 & 0 & \varepsilon_{zz} \end{pmatrix}$. However, realizing a TO medium with this matrix is a difficult task. To overcome the difficulty, we pay attention to the ε_{yy} profile alone. In Fig. 2(a) ε_{yy} profile is plotted

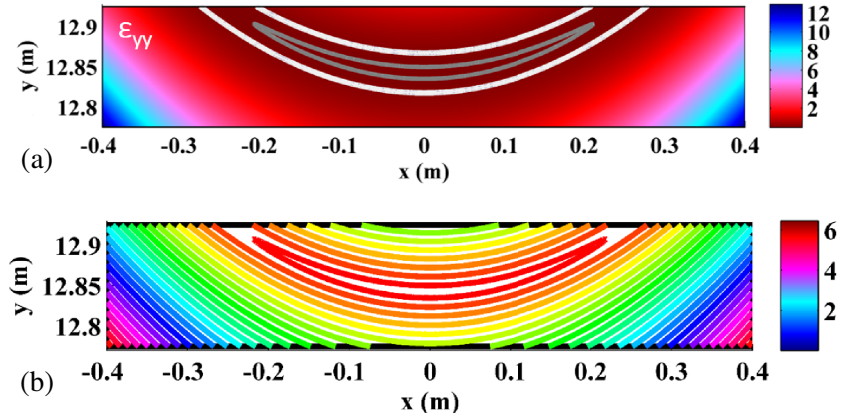

Figure 2. (a) Dielectric permittivity (Eq. (6) is scaled down by a factor of 10) and (b) corresponding refractive index profiles of a proposed TO medium.

by scaling down a factor of 10. It has interesting spatial contours with curved features with dielectric constant ranging from 0.09 to 12. From Fig. 2(a), one can note that along any given contour, the permittivity value is a constant. Suppose that a material has a dielectric profile as shown in Fig. 2(a), it may suffice to confine e-m modes due to its sub-wavelength spatial variation with curved features. Fig. 2(b) shows the corresponding refractive index profile. We attempt to utilize the contours of ε_{yy} profile for e-m confinement, and hence we restrict our TO medium to be non-magnetic with the spatial variation of dielectric constant alone.

3. SQUEEZED MODE CONFINEMENT IN A TO CAVITY

It is observed from Fig. 1(b) that the entire space is under the coordinate transformation. However, our approach is to take the specific region of the TO space and utilize it for different e-m applications. Hence from Fig. 1(b), the region at the position of the upper curvature centered at (0, 12.85 m) and spreading out over the area of 0.8 m × 0.15 m is employed for the cavity realization, as this regime has many squeezed contours of refractive indices as shown in Fig. 2(b). We identify that this selected regime acts as a cavity resonator because in this selected regime, the refractive index values span from 0.091 to 3.533, and due to the presence of sub-zero index to the higher index gradient in the profile, e-m waves are expected to confine and form an e-m mode within the smaller contours of the TO rectangular geometry.

To find out the characteristic modes of the proposed TO geometry, eigenmode calculations are carried through finite-element method based COMSOL Multiphysics [27]. In eigenmode analysis, the TO geometry is assigned with perfect electric boundary conditions (PEC) described by $\hat{n} \times \vec{E} = \vec{0}$. Figs. 3(a)–(c) show the mode profile of the TO geometry. To compare the squeezing area aspect, the mode profile of an air-filled metallic cavity of same dimensions is shown in Figs. 3(d)–(f). It is evident that the characteristic modes of an air-filled metallic cavity cannot show any spatial compression in it. On the other hand, for the TO geometry, the characteristics modes are flattened horizontally and squeezed vertically as shown in Figs. 3(a)–3(c). At this point, it is useful to emphasize that resonant modes of air-filled. TO cavities are different, and they have no correspondence with each other, i.e., air cavity modes are not compressed by using TO space. Rather, the modes of TO cavity are unique due to the designed permittivity profile.

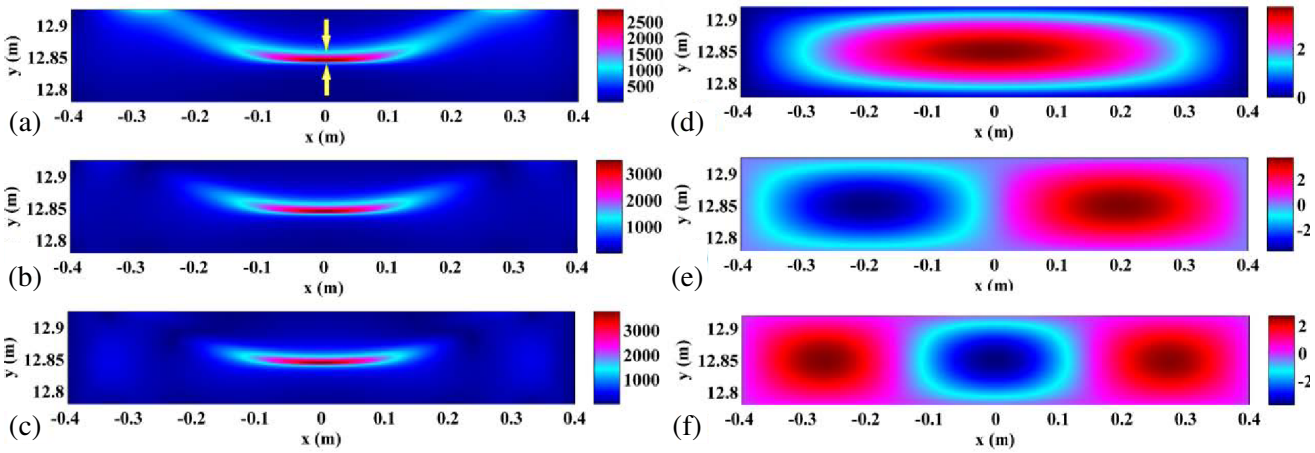

Figure 3. (a)–(c) e-m modes of a TO cavity at 0.3371 GHz, 0.6827 GHz and 0.9777 GHz respectively. (d)–(f) e-m modes of air filled metallic cavity at 1.0167 GHz, 1.0673 GHz, and 1.1466 GHz, respectively.

To compare the degree of squeezing, electric field intensity ($|\vec{E}|^2$) of the characteristic e-m modes is scanned horizontally and vertically with respect to a point at (0, 12.845 m) for both the TO and air-filled metallic cavities, and are plotted in Fig. 4. The vertical spatial width (full-width at half-maximum-FWHM) of an e-m mode of a TO cavity computed at 0.9777 GHz is 0.0062 m, whereas the

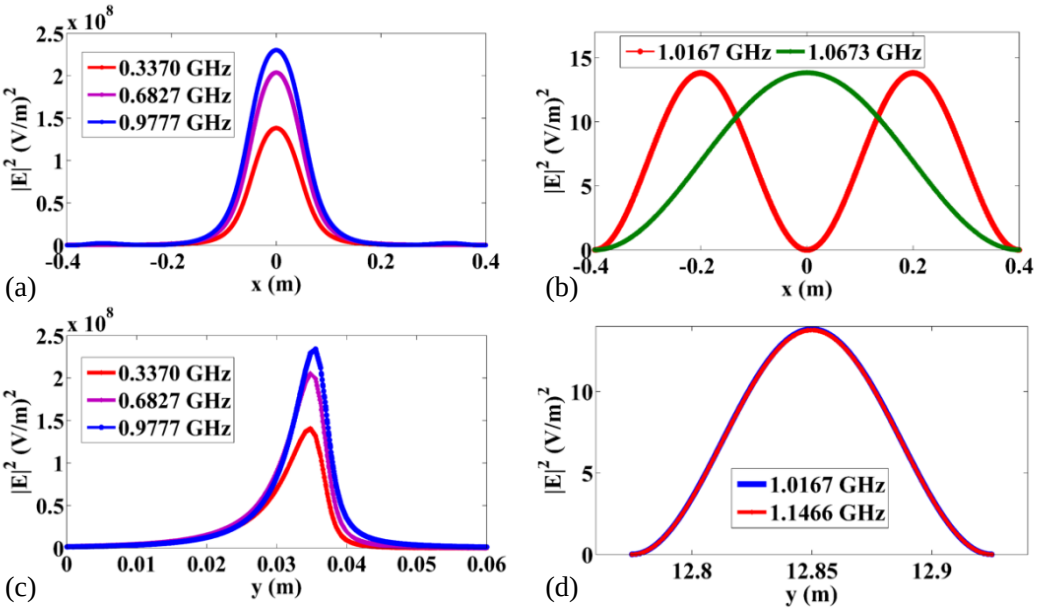

Figure 4. (a) and (b) horizontal, and (c) and (d) vertical scanning of electric field intensity profiles of various e-m modes of TO and air-filled metallic cavities with respect to a point at (0, 12.845 m), respectively.

vertical FWHM of the fundamental mode (at 1.0167 GHz) of an air-filled cavity is 0.0750 m. Thus the vertical FWHM of the e-m mode of a TO cavity corresponds to a vertical squeezing of the dimension of $\lambda/49.48$.

In the case of a horizontal scanning ($y = 12.845$ m line at $x = 0$), the FWHM of an e-m mode of a TO cavity computed at 0.9777 GHz is 0.1349 m, whereas for an air-filled metallic cavity, the horizontal FWHM of an e-m mode at 1.0167 GHz is 0.4000 m. The horizontal FWHM of the flattened e-m mode of TO cavity is of the dimension of $\lambda/2.28$.

Both the vertical and horizontal FWHMs of an e-m mode of a TO cavity suggests the squeezed confinement along vertical direction, and this significant feature is mainly due to the refractive index gradient profile of the TO medium.

To further quantify the degree of squeezing, an effective mode area ($A_{eff} = \frac{(\iint |E(x,y)|^2\, dxdy)^2}{\iint |E(x,y)|^4\, dxdy}$) is calculated for both TO cavity and air-filled metallic cavity, and they are listed in Table 1. It is found that at least 10 times reduction in the effective mode area is witnessed for the characteristic modes of TO cavity in comparison with the air-filled metallic cavity.

From the proposed TO cavity, one can use the squeezed cross-section of the cavity mode for

Table 1. Comparison between TO and air-filled metallic cavities of dimensions 0.8 m × 0.15 m.

Type of Cavity	Resonant Mode Frequency (GHz)	Effective Mode Area (m^2)
TO cavity	0.3370	0.0140
	0.6827	0.0080
	0.9777	0.0069
Air-filled metallic cavity	1.0167	0.0566
	1.0673	0.0660
	1.1466	0.0789

a selective e-m interaction including heating and material characterization. In a typical cavity perturbation technique, a dielectric/magnetic sample is kept at the maximum electric field of the cavity mode, and if the size of the mode is tiny, it will be useful for targeted material treatment.

4. APPLICATION: ELECTROMAGNETIC THERMAL CO-SIMULATION OF TARGETED MATERIAL HEATING

To demonstrate the heating application, eigenmode results are validated against full-wave computations by externally exciting a cavity with an e-m source, and thermal co-simulations are carried out subsequently. Fig. 5(a) shows the electric field norm plot of the TO cavity at 0.9651 GHz for a TM line source excited at the angle of 35°. It may be noted that the resonant mode in a cavity can be excited for any incident angle as the mode excitement is independent of the position of the incident source. However to minimize perturbation losses due to loading of heating material into the cavity, optimized source's position is chosen. It is observed that both the eigenmode and full-wave e-m wave computations verify the spatially squeezed e-m modes of the proposed TO cavity with the slight shift in the resonant frequencies (Table 1).

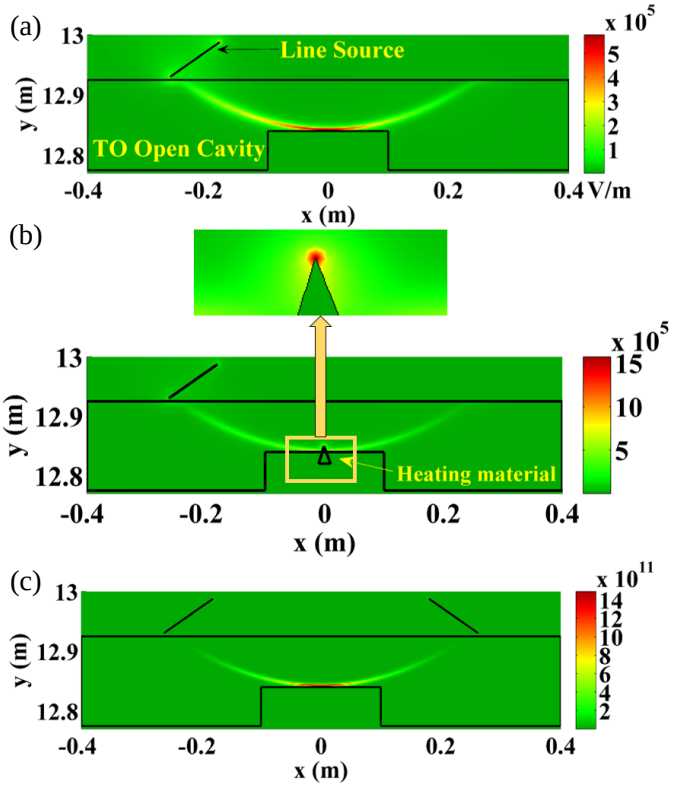

Figure 5. (a) Electric field norm of the TO cavity mode at 0.9651 GHz for ad TM polarized incident wave. Line source emitting TM wave is inclined at angle of 35°. (b) Electric field norm of the TO cavity mode at 0.9651 GHz after loading a triangular heating object into the TO cavity. The field perturbation due to the heating object is highlighted separately. (c) Electric field norm for twin-beam excitations at 0.9651 GHz.

To utilize this mode confinement for material heating, a cone object with dimensions of base length 2 cm and height 1.9 cm is taken as a heating object, and it is loaded at the mode's confinement area of the cavity as shown in Fig. 5(b). Fig. 5(b) shows the electric field norm plot for a triangular dielectric heating object loaded into the TO cavity at 0.9651 GHz, for a TM line source excited at angle of 35°. The incident e-m wave's peak electric field strength is kept as $5e^4$ V/m. It is observed that the presence of heating object does not perturb the mode confinement drastically. This is evident from the field plot

highlighted in Fig. 5(b), where around the tip of the heating object, e-m mode is concentrated. It is further interesting to note that instead of a single line-source, one can also use multiple e-m sources to excite the cavity mode. This is illustrated in Fig. 5(c), where twin line sources of TM polarization (each with peak electric field strength of $5e^4$ V/m) excite the cavity, and squeezed mode confinement is observed.

The heating due to e-m beam confinement is studied through electromagnetic thermal co-simulation [28]. The e-m thermal co-simulation involves a two-step procedure, where at first, the harmonic field solution is obtained by solving a Maxwell's wave equation, and in the second step time-domain studies are performed by solving the heat transfer differential equation by considering cavity mode's e-m energy as a heat source. The partial differential equations governing e-m thermal co-simulations are given as

$$\begin{aligned} &\nabla \times \mu_r^{-1}(\nabla \times \vec{E}) - k_0^2 \left(\varepsilon_r - j\sigma/\left(\omega\varepsilon_0\right)\right)\vec{E} = 0, \\ &\rho C_p \frac{\partial T}{\partial t} + \rho C_p \vec{U}_{\text{trans}} \cdot \nabla T = \nabla \cdot (K\nabla T) + Q, \end{aligned} \tag{11}$$

where μ_r is the relative permeability; k_0 is the wavenumber; ρ is the density of the heating material; C_p is the specific heat capacity at constant pressure; T is the Temperature; K is the thermal conductivity; $\vec{U}_{\text{trans}}$ is the velocity vector which denotes the rate of heat flow per unit cross-sectional area; and Q is the heat source. Thermal properties of a heating cone object are taken as follows: $\varepsilon_r = 2.829 - j*0.174$, $C_p = 2.821 \times 10^3 \text{J kg}^{-1}\text{K}^{-1}$, $K = 0.17\,\text{W/mK}$, and $\rho = 928\,\text{kg/m}^3$ [28]. In solving the heat transfer equation, boundaries of the heating medium are treated with the thermally insulating boundary condition given as $\hat{n} \cdot (K\Delta T) = 0$, where $\hat{n}$ is the unit normal vector, and ΔT is the temperature gradient.

Figure 6 shows the e-m thermal co-simulation results for single and dual line sources exciting the TO cavity with a peak electric field strength of $5e^4$ V/m at 0.9651 GHz. For a single (dual) line source, a heating rate of 2.35°C/s (11°C/s) is observed. The rise in temperature over a time follows a parabolic trend for both single and dual beam excitations. However, higher heating rates of 90°C/min (single beam) and 138°C/min (twin beams) are witnessed. The temperature distribution profile of a heating object at 60 s is shown in the inset of Fig. 6 for dual beam excitations. It is observed that from the tip to the bottom of the cone, most of the heating is witnessed within 0.5 cm from the tip (magnified part of the cone object is highlighted in the inset of Fig. 6).

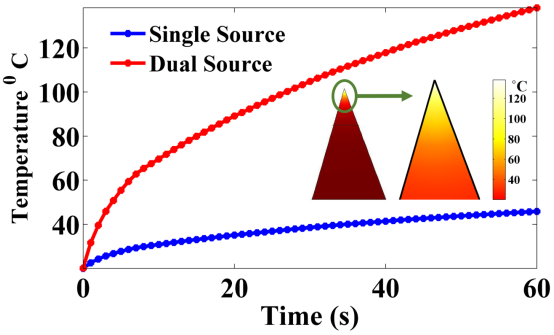

Figure 6. Time dependence of temperature rising of a heating object due to single and dual e-m beams. Inset shows temperature distribution of a cone object at 60 s for twin beam excitations.

5. DISCUSSION ON THE PRACTICAL REALIZATION OF A TO CAVITY

The spatially squeezed e-m modes of a TO cavity are due to the refractive index variation. Hence, the replication of refractive index at all the points in the coordinate space will reconstruct the cavity. However, achieving such spatial variation is not an easy task. Usually one may go for a cell approximation, in which the designed TO medium is approximated by a rectangular grid [29], where

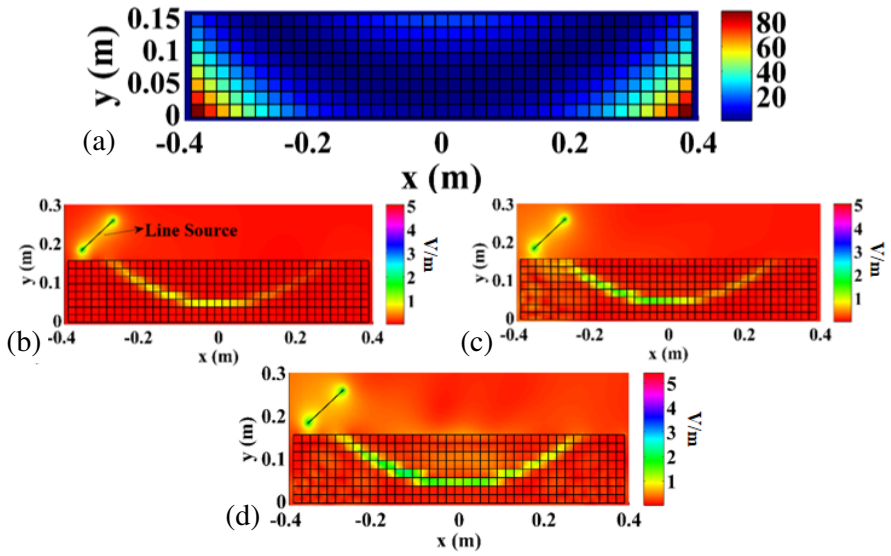

Figure 7. (a) Grid representation of a TO medium responsible for squeezed e-m modes. Each unit cell size is 0.02 m × 0.02 m. (b)–(d) e-m modes of a cell approximated TO cavity at 0.3416 GHz, 0.5833 GHz and 0.825 GHz respectively.

at each grid point, a material with required refractive index is kept. To practically realize the curved refractive index profile proposed in the work, we have simplified the TO medium as in Fig. 6(a). It consists of 312 square unit cells, where each unit cell dimension is 0.02 m × 0.02 m. Each unit cell is assigned with the uniform relative permittivity values corresponding to permittivity values at the center of the unit cell. From Fig. 7(a), one can note that each square grid of given color indicates the constant value of a relative dielectric permittivity. Hence, the demonstrated confinement can be achieved with this approximated cell based TO cavity. Full-wave e-m results for the approximated TO cavity are shown in Figs. 7(b)–(d) where fundamental modes of the TO cavity are in agreement with the eigenmode analysis (Table 1) and full-wave computations (Sec. 4)). Apart from this computation, it is further useful to mention the types of materials available for filling each square grid with required refractive index values varying from sub-zero to 3.5. As far as sub-zero refractive index values are concerned, metamaterials (MTM) are desirable. A sub-wavelength MTM unit cell size of $\lambda/10$ [30] was practically realized at microwave/THz frequencies previously. In the case of higher refractive index values, periodic array of photonic crystals can be attempted [31]. Moreover, microwave/THz material with a refractive index varying from 2 to 3.6 can be molded along a given curve using ink-jet and 3-D printing fabrication techniques [32, 33]. It has been recently demonstrated that the variation of infill percentage of 3-D printing dielectric moldings provides necessary permittivity variations [34]. Therefore, we anticipate that the observed squeezed e-m modes of a proposed TO cavity are realizable at microwave/THz frequencies.

6. CONCLUSIONS

Spatially squeezed e-m modes of a cavity resonator formed by modified TO medium were reported. The proposed TO medium comprises layered contours of refractive index profiles, where e-m mode was confined within the contours. The material parameters of the proposed TO medium are non-magnetic and simplified with the spatial variation of dielectric permittivity alone. The effective mode area of the e-m modes of a TO cavity is at least 10 times smaller than the effective mode area of the e-m modes of an air-filled metallic cavity. The confined e-m mode of a TO cavity is flattened and squeezed along horizontal and vertical dimensions, respectively. The vertical FWHM of the e-m mode of a TO cavity is $\lambda/49$. For an application aspect, squeezed e-m modes of a TO cavity were used for targeted material heating, and it was demonstrated based on e-m thermal co-simulations. We have found that

a tiny dielectric material placed at the squeezed part of the cavity mode was heated rapidly with the temperature rise of 2.35°C/s (11°C/s) for the single (dual) e-m source excitations with the moderate peak electric field strength of $5e^4$ V/m. The results of grid-cell approximation are in agreement with the eigenmode analysis and full-wave computations, and thus it is indicated that the proposed TO cavity is practically realizable at microwave frequencies. We further anticipate that the demonstrated work may accelerate TO research by coupling electromagnetic and heat transfer domains for novel photonic device realizations.

Declaration of Competing Interest

The authors declare that they have no known competing financial interests or personal relationships that could have appeared to influence the work reported in this paper.

ACKNOWLEDGMENT

This work was funded by the Department of Science and Technology, Ministry of Science and Technology, India (DST/INSPIRE/04/2015/002420).

REFERENCES

1. Vučković, J., "Quantum optics and cavity QED with quantum dots in photonic crystals," Note 2013, Stanford University, 2013.
2. Ramakrishna, S. A., S. Guenneau, S. Enoch, G. Tayeb, and B. Gralak, "Confining light with negative refraction in checkerboard metamaterials and photonic crystals," *Phys. Rev. A*, Vol. 75, 063830, 2007.
3. Yi, J., Z. Shi, D. Li, C. Liu, H. Sun, L. Zhu, X. Chen, and S. N. Burokur, "A metamaterial lens based on transformation optics for horizontal radiation of OAM vortex waves," *J. Appl. Phys.*, Vol. 129, 2021.
4. Tanaka, Y., J. Upham, T. Nagashima, T. Sugiya, T. Asano, and S. Noda, "Dynamic control of the Q factor in a photonic crystal nanocavity," *Nature Mater.*, Vol. 6, 862–865, 2007.
5. Kishk, A. A., A. W. Glisson, G. P. Junker, W. M. Ave, and E. Segundo, "Bandwidth enhancement for split cylindrical dielectric resonator antennas," *Progress In Electromagnetics Research*, Vol. 33, 97–118, 2001.
6. Ward, A. J. and J. B. Pendry, "Refraction and geometry in Maxwell's equations," *J. Mod. Opt.*, 773–793, 1996.
7. Teixeira, F. L., H. Odabasi, and K. F. Warnick, "Anisotropic metamaterial blueprints for cladding control of waveguide modes," *J. Opt. Soc. Am. B*, Vol. 27, 1603, 2010.
8. McCall, M., J. B. Pendry, V. Galdi, Y. Lai, S. A. R. Horsley, J. Li, J. Zhu, R. C. Mitchell-Thomas, O. Quevedo-Teruel, P. Tassin, V. Ginis, E. Martini, G. Minatti, S. Maci, M. Ebrahimpouri, Y. Hao, P. Kinsler, J. Gratus, J. M. Lukens, A. M. Weiner, U. Leonhardt, I. I. Smolyaninov, V. N. Smolyaninova, R. T. Thompson, M. Wegener, M. Kadic, and S. A. Cummer, "Roadmap on transformation optics," *J. Opt.*, Vol. 20, No. 6, United Kingdom, 2018.
9. Leonhardt, U. and T. G. Philbin, "Chapter 2 Transformation optics and the geometry of light," *Prog. Opt.*, Vol. 53, 69–152, 2009.
10. Van Dantzig, D., "The fundamental equations of electromagnetism, independent of metrical geometry," *Math. Proc. Cambridge Philos. Soc.*, Vol. 30, 421–427, 1934.
11. Teixeira, F. L. and W. C. Chew, "Differential forms, metrics, and the reflectionless absorption of electromagnetic waves," *Journal of Electromagnetic Waves and Applications*, Vol. 13, 665–686, 1999.
12. Deschamps, G. A., "Electromagnetics and differential forms," *Proc. IEEE*, Vol. 69, 676–696, 1981.
13. Rahm, M., D. Schurig, D. A. Roberts, S. A. Cummer, D. R. Smith, and J. B. Pendry, "Design

of electromagnetic cloaks and concentrators using form-invariant coordinate transformations of Maxwell's equations," *Photonics Nanostructures — Fundam. Appl.*, Vol. 6, 87–95, 2008.

14. Pendry, J. B., D. Schurig, and D. R. Smith, "Controlling electromagnetic fields," *Science*, Vol. 312, 1780–1782, 2006.
15. Yang, J., M. Huang, C. Yang, J. Peng, and R. Zong, "Metamaterial electromagnetic superabsorber with arbitrary geometries," *Energies*, Vol. 3, No. 7, 1335–1343, 2010.
16. Vasantharajan, G., N. Yogesh, and V. Subramanian, "Beam steering based on coordinate transformation of Fermat spiral configurations," *AIP Adv.*, Vol. 9, 075217, 2019.
17. Fernandez-Domınguez, A. I., S. A. Maier, and J. B. Pendry, "Collection and concentration of light by touching spheres: A transformation optics approach," *Phys. Rev. Lett.*, Vol. 105, 266807, 2010.
18. Tsang, M. and D. Psaltis, "Magnifying perfect lens and superlens design by coordinate transformation," *Phys. Rev. B*, Vol. 77, 035122, 2008.
19. Dehdashti, S., H. Wang, Y. Jiang, Z. Xu, and H. Chen, "Review of black hole realization in laboratory base on transformation optics," *Progress In Electromagnetics Research*, Vol. 154, 181–193, 2015.
20. Kadic, M., G. Dupont, S. Enoch, and S. Guenneau, "Invisible waveguides on metal plates for plasmonic analogs of electromagnetic wormholes," *Phys. Rev. A* Vol. 90, 043812, 2014.
21. Rahm, M., S. A. Cummer, D. Schurig, J. B. Pendry, and D. R. Smith, "Optical design of reflectionless complex media by finite embedded coordinate transformations," *Phys. Rev. Lett.*, Vol. 100, 063903, 2008.
22. Zhou, J., M. Li, L. Xie, and D. Liu, "Design of a new kind of polarization splitter based on transformation optics," *Optik*, Vol. 122, 1672–1675, 2011.
23. Haddad, H., R. Loison, R. Gillard, A. Harmouch, and A. Jrad, "A combination of transformation optics and surface impedance modulation to design compact retrodirective reflectors," *AIP Adv.*, Vol. 8, 025114, 2018.
24. Pakniyat, S., S. Jam, A. Yahaghi, and G. W. Hanson, "Reflectionless plasmonic right-angled waveguide bend and divider using graphene and transformation optics," *Optics Express*, Vol. 29, No. 6, 9589–9598, 2021.
25. Xu, L. and H. Chen, "Conformal transformation optics," *Nat. Photonics*, Vol. 9, 15–23, 2014.
26. Chang, Z., X. Zhou, J. Hu, and G. Hu, "Design method for quasi-isotropic transformation materials based on inverse Laplace's equation with sliding boundaries," *Optics Express*, Vol. 18, No. 6, 6089, 2010.
27. Whiteman, J. R., *The Mathematics of Finite Elements and Applications*, John Wiley and Sons, Chichester, 1998, http://www.comsol.com.
28. Yogesh, N., Q. Yu, and Z. Ouyang, "Single- and multi-beam confinement of electromagnetic waves in a photonic crystal open cavity providing rapid heating and high temperatures," *Photonics Nanostructures — Fundam. Appl.*, Vol. 15, 89–98, 2015.
29. Cao, Y., J. Xie, Y. Liu, and Z. Liu, "Modeling and optimization of photonic crystal devices based on transformation optics method," *Optics Express*, Vol. 22, 2725–2734, 2014.
30. Yan, S. and G. A. E. Vandenbosch, "Compact circular polarizer based on chiral twisted double split-ring resonator," *Appl. Phys. Lett.*, Vol. 102, 103503, 2013.
31. Yogesh, N. and V. Subramanian, "Spatial beam compression and effective beam injection using triangular gradient index profile photonic crystals," *Progress In Electromagnetics Research*, Vol. 129, 51–67, 2012.
32. Zhou, N., C. Liu, J. A. Lewis, and D. Ham, "Gigahertz electromagnetic structures via direct ink writing for radio-frequency oscillator and transmitter applications," *Adv. Mater.*, Vol. 29, No. 15, 1605198, 2017.
33. Velasco-Hogan, A., J. Xu, and M. A. Meyers, "Additive manufacturing as a method to design and optimize bioinspired structures," *Adv. Mater.*, Vol. 30, No. 52, 1800940, 2018.
34. Poyanco, J. M., F. Pizarro, and E. Rajo-Iglesias, "Wideband hyperbolic flat lens in the Ka-band based on 3D-printing and transformation optics," *Appl. Phys. Lett.*, Vol. 118, 2021.